

Investigation of interaction of the Lamb wave with delamination type defect in GLARE composite using air-coupled ultrasonic technique

Andriejus Demčenko, Egidijus Žukauskas, Rymantas Kažys, Algirdas Voleišis
Ultrasound Institute, Studentų Str. 50, LT-51368 Kaunas, Lithuania, andriejus.demcenko@ktu.lt

Ultrasonic NDT is one of the most frequently applied methods for testing of composite materials. A measured wave velocity gives information about composite properties. A change in the velocity indicates possible presence of a defect. Application possibilities of air-coupled ultrasonic technique for investigation of the Lamb wave propagation in the composite material and the numerical simulations of the Lamb wave interaction with the delamination type defect are presented. The Lamb wave velocities are measured in delaminated and defect-free areas of the composite material GLARE. The delamination position influence on the Lamb wave propagation velocity is investigated experimentally and numerically.

1 Introduction

Strong attention is paid on testing and measurement of various aerospace structures and materials such carbon / glass fibre reinforced plastics, honeycombs and glass fibre metal laminates. An air-coupled ultrasonic measurement technique has a great potential for investigation of those materials in manufacturing and maintenance.

During maintenance of a product only one-side access to the object under a test usually is possible, so Lamb waves have to be employed in the air-coupled ultrasonic technique.

The objective of this work was an investigation of the Lamb wave A_0 mode interaction with a delamination type defect in GLARE3-3/2 composite material using air-coupled ultrasonic technique. The defect selected was approximately 4 times larger then the wavelength.

The structure of the GLARE3-3/2 composite and the position of the delamination type defect are shown in Figure 1.

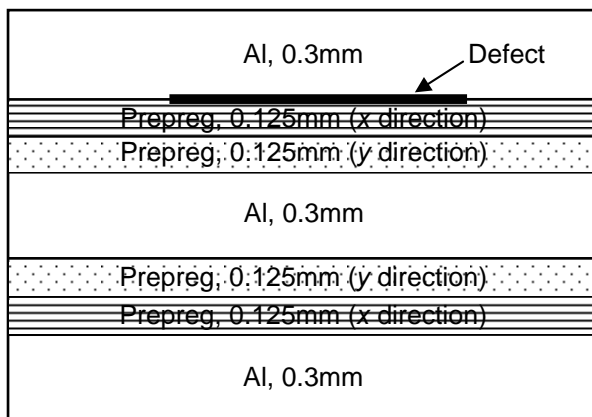


Figure1: The structure of the GLARE3-3/2 composite and the position of the defect

The GLARE3-3/2 composite material is 1.4mm thick glass fibre metal laminate. It consists of three 0.3mm aluminium alloy layers and two layers of 0.25mm thickness prepreg. Each prepreg layer consists of two glass fibre plies laid perpendicularly to each other and glued with epoxy resin. The artificial 25mm circular delamination type defect between the first aluminium layer and the prepreg was done from sealed Teflon.

2 Theory background

2.1 The Lamb waves in plate-like structures

It is well known that theoretically an infinite number of Lamb waves modes exist. If a structure is a single layer plate, the governing phase velocity dispersion curves can be obtained from transcendental equations [1]. The dispersion curves for multilayered structures can be calculated using various matrix methods [2 - 6]. When the plate is surrounded by a liquid or a solid, an energy leakage occurs from the plate to the surrounding media. In this case attenuation acts in the system and the wave's amplitude is damped in the plate. Due to the leakage it is possible to carry out measurements with leaky Lamb waves in air as well. The phase velocity and the attenuation dispersion curves predicted for the GLARE3-3/2 composite in air using the global matrix method [5] are presented in Figure 2 and 3.

The most important and widely used for measurements are the lowest order symmetric S_0 and antisymmetric A_0 Lamb waves modes. In our investigation frequencies range (210kHz) only those two modes can be excited. In the previous investigation of the A_0 mode phase velocity in the GLARE3-3/2 panel it was shown that with a pair of air-coupled piezoceramic transducers only antisymmetric A_0 mode in GLARE3-3/2 panel can be received [7]. It may be also explained

by the energy leakage to the surrounding media. It is seen from Figure 3 that S_0 mode attenuation is very low (less than 2.22×10^{-3} db/m) at 210kHz when A_0 mode has 0.52db/m energy leakage to air at the same frequency.

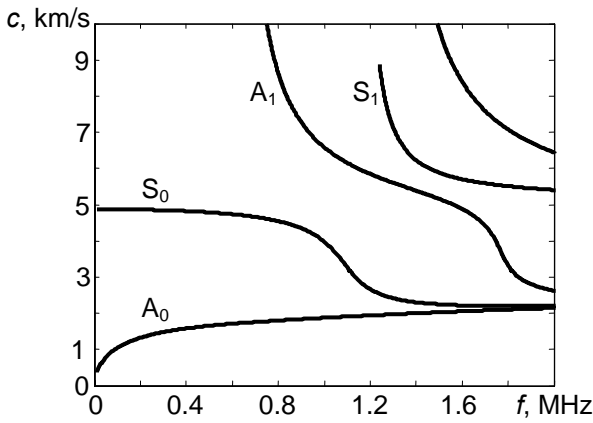


Figure 2: The phase velocity dispersion curves in the GLARE3-3/2 panel

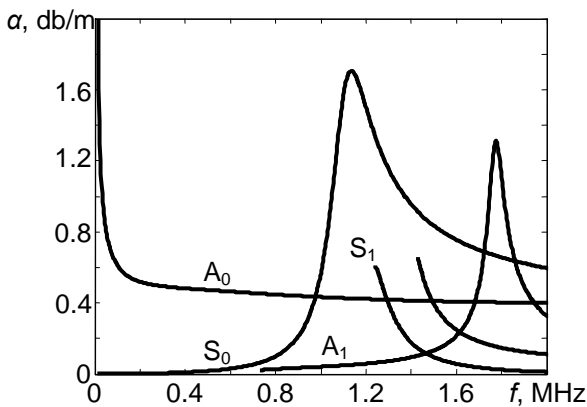


Figure 3: The attenuation dispersion curves in air

2.2 The wave interaction with defect

An attention was paid to interaction of the Lamb waves with various types of defects by many researchers [8-15]. The investigations were carried out using contact transducers or embedded sensors and there was no information about the scattered wave-field leakage into the surrounding media. Summarizing the published results, it may be shown that during the Lamb wave interaction with a defect scattering and mode conversions occurs.

In our case a part energy of the A_0 Lamb wave mode transforms into S_0 mode, but the S_0 Lamb wave mode has too small leakage into air, so it can not be detected by the air-coupled ultrasonic technique. So, in presence of a defect only change in wave propagation velocity or change in signal amplitude can be detected.

When the A_0 Lamb wave mode propagates around the defect in the composite (Figure 1) the part of the wave energy propagates in the first aluminium layer over the defect and the part of the wave energy propagates under the defect. In this case there are three different velocities of the A_0 Lamb wave mode: in defect-free area, in areas over and under the delamination type defect. The predicted phase velocity changes are shown in Figure 4.

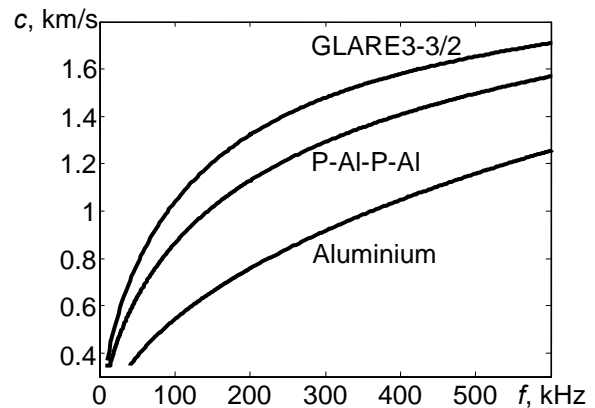


Figure 4: The A_0 mode dispersion curves in the composite GLARE3-3/2, prepreg-aluminium-prepreg-aluminium (P-Al-P-Al) structure and 0.3mm thickness aluminium

Modelling results show that strong velocity degradation occurs when the wave propagates through the aluminium layer and the change of the velocity must be easy detectable and significant. Not so strong velocity change can be fixed when the wave propagates under the defect. The numerical simulations and experimental verification results of the wave interaction with the defect are presented in next sections.

3 The numerical simulations

3.1 The numerical model

The 2D numerical simulations of the wave interaction with the defect were carried out with Wave2000 software. The delamination type defect was simulated as 25mm width thin vacuum gap between aluminium and prepreg layer. A virtual 10mm width strip-like transmitter was used to excite the A_0 Lamb wave mode in the composite. The excitation angle was selected to be 12° and the transmitter was excited by a 3 cycles 800V 210kHz sine burst. The transducers and the plate configuration are presented in Figure 5. The distance A between the transmitter and the plate was 1.8mm. As a receiver the virtual 10mm width array consisting of 10 strip-like elements was used. The width of each

element was 1mm. The array was orientated parallelly to the surface of the composite and the distance B between the composite panel and the array was 1mm. The manipulation with a time delay for each element of the array gave possibilities to investigate the received signals at various angles with different types of apertures including non-uniform and focusing apertures.

The distance C between the transducer and the receiver was selected to be 30mm. It was enough to receive the clear leaky Lamb wave signal of the 3 cycles at the frequency of 210kHz. Of course, the shorter distance would give a better spatial resolution, but a direct acoustic signal from the transducer to the receiver would distort the leaky Lamb wave signal.

Simultaneously moving the transmitter and the receiver, the A_0 mode leakage was received with the array. The scanning was carried out in front of, over and behind the defect with a scanning step of 1mm. In this way a synthetic B-scan was formed from the collected data.

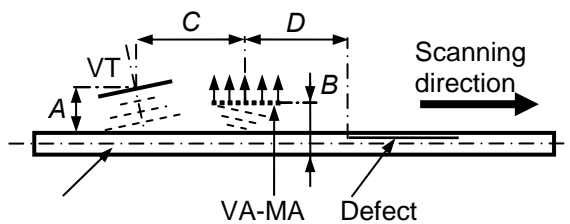


Figure 5: The arrangement of the transducers and the defect for the B-scan simulation: VT is the virtual transmitter and VA-MA is the virtual receiver with the multiple outputs

3.2 The simulation results

In Figures 6-8 the typical snapshots of the displacement fields are presented. It is seen that the energy leakage in front of the defect is symmetric in the both sides of the structure. Crossing the delaminated area the Lamb wave mode conversions occurs and in the structures, aluminium and P-Al-P-Al, the two A_0 Lamb wave modes with the different velocities propagate. Over the delaminated area in the aluminium layer multiple reflections and the scattering of the A_0 mode occur. The multiple reflections in the structure under the defect can not be seen.

In Figure 9 the simulated B-scan is shown when the signals received with the array were phased at 12 degree angle. The vertical axis x represents the scanned distance in millimetres and the horizontal axis t shows the time of the flight of the signals. The coding in the colours represents the amplitudes of the signals. The horizontal lines mark a doubled defect area. The doubling can be explained by the defect shielding of

the transducers. First of all the receiver was scanned over the defect. In the aluminium layer the A_0 mode propagated slower than in the composite GLARE and the time delay increased. The estimated maximum change of the time delay was $5\mu\text{s}$. The degradation of the signals amplitudes was caused by the change of the wave leakage angle, which must satisfy a Snell law. During scanning the excitation and reception angles were fixed, so the reception angle was not optimal. The same situation also was with the transmitter.

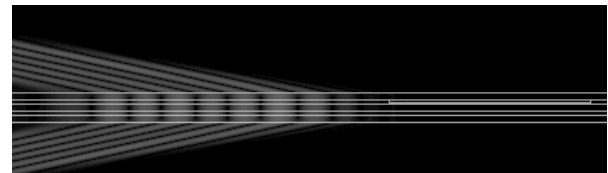


Figure 6: The snapshot of the wave displacement field before the defect

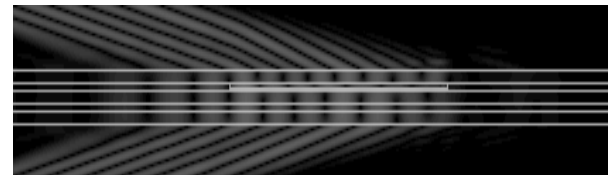


Figure 7: The snapshot of the displacement fields of the two A_0 Lamb wave modes with the different velocities

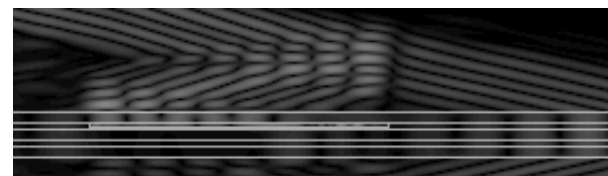


Figure 8: The snapshot of the displacement field over the defect

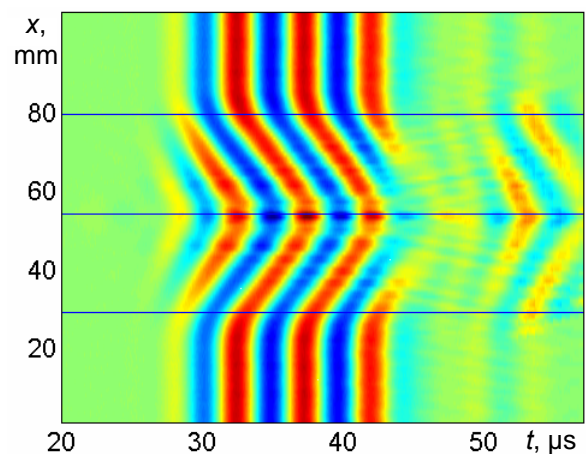


Figure 9: The simulated B-scan

4 The experimental verification

4.1 The measurement system

Air-coupled unfocused planar transducers, manufactured in the Ultrasound Institute (UI) of Kaunas University of Technology were used in the experimental measurements. 1-3 piezocomposite transducers had the resonance frequency 210kHz, the dimensions were 10×20mm, the thickness 7.2mm. Rods were 1.4×1.4mm, kerfs 0.6mm, so percentage of PZT ceramic was 50% and impedance was about 14MRayl. The first $\lambda/4=2.4\text{mm}$ matching layer was of epoxy with cork dust with the 2.1MRayl impedance. The final $\lambda/4=1.0\text{mm}$ matching layer was made of cork. Its density was 0.25g/cm^3 and impedance was 0.15MRayl. The amplitude of the transducer with matching layer was 16.5 times greater than without the matching. The transmitter was excited by a 1 cycle 800V 210kHz rectangular burst using the air-coupled ultrasonic measurement system controlled by a personal computer and manufactured in UI. The receiver was connected to a 13.4db preamplifier (UI) and after it the signals were amplified, digitized and averaged by the air-coupled ultrasonic measurement system. The total gain was 66.4db. The sampling frequency was 25MHz and the averaging was from the 128 signals. After averaging the signals were transmitted through USB2 and were stored in the personal computer for data analysis.

The configuration of the transducers was close to the simulation configuration. The longer sides of the transducers were oriented perpendicularly to the scanning direction. The distances A and B were approximately 3mm. The distance C was 30mm.

4.2 The measurement results

Figure 10 shows the experimental B-scan. The B-scan ranges 1mm – 25mm and 75mm – 100mm are in the defect-free areas. The delaminated zone has delayed and lower amplitude signals and they can be seen in the range 25mm – 75mm. The range is twice large than the diameter of the defect. At the centre of the B-scan ($x=48\text{mm}$) the amplitude of the signals increased due to the resonance of the waves and it well agrees with the simulated data.

The signals in the defect free area and in the delaminated area are presented in Figure 11. The largest estimated time delay between the defect-free ($x=10\text{mm}$) and delaminated area ($x=48\text{mm}$) is $4.38\mu\text{s}$. The difference of the time delay was found between the maxima of the signals. The estimated difference pick-to-pick of the signals amplitudes is 0.1904V.

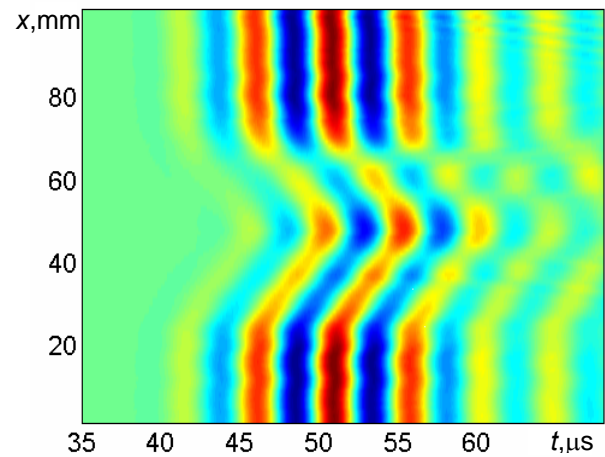


Figure 10: The experimental B-scan

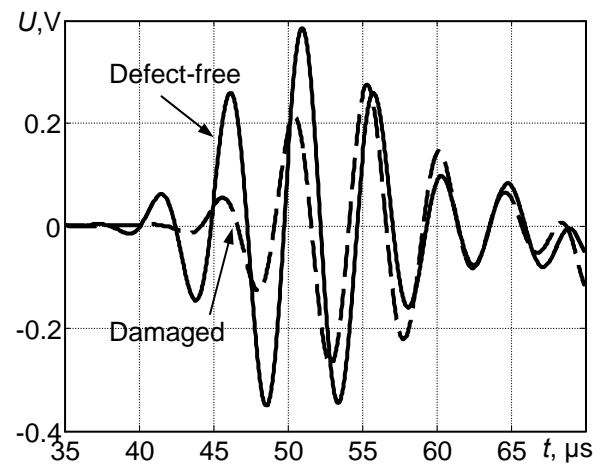


Figure 11: The signal in the defect-free area when $x=10\text{mm}$ and the signal in delaminated area when $x=48\text{mm}$

4.3 Air-coupled visualisation of the defect

Two different C-scans of the same defective area are presented in Figure 12 and 13 at the same scale. The horizontal axis shows the scanned distance in x direction and the vertical axis shows the distance in y axis. The coding in colours shows the change of the amplitude or the change of time of flight respectively to the C-scan.

It is seen that the C-scan in the time domain is more accurate and it gives dimensions closer to the true size of the defect, but it does not display information about the waves resonances in the delaminated area which can be clearly seen in the amplitude C-scan and in the previous B-scans.

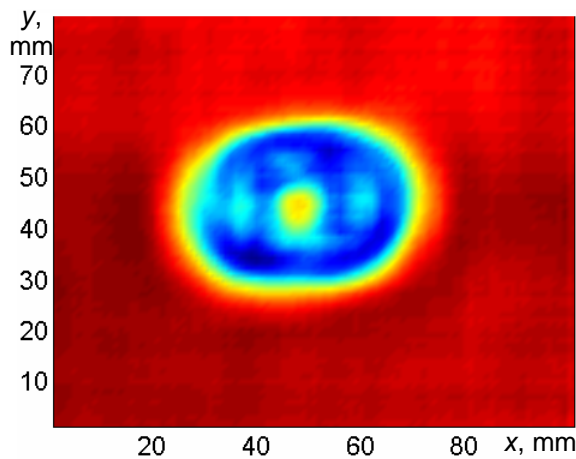


Figure 12: The amplitude C-scan of the damaged area

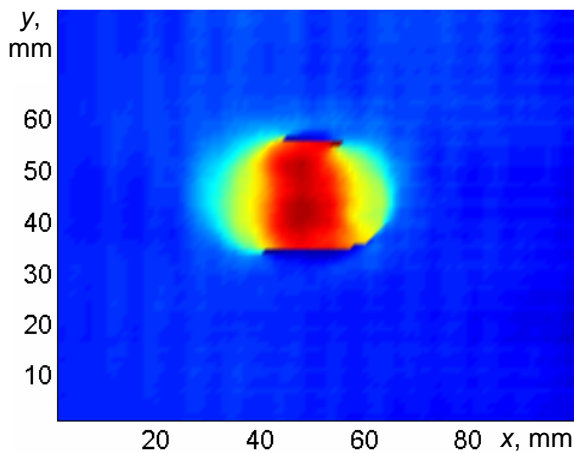


Figure 13: The time of flight C-scan of the damaged area

5 Discussion

The air-coupled ultrasonic measurement technique can be used for accurate investigation and testing of various types of the materials, but it is not suitable for the fundamental investigations of the waves interactions with the non-homogeneities or defects in the structures. The loss of information occurs using the air-coupled ultrasonic technique due a mode conversion phenomenon in defective areas. In our case the A_0 Lamb wave mode generates the S_0 Lamb wave mode, which in a low frequency range has too low energy leakage into air and due to this it can not be detected with the air-coupled ultrasonic technique. When the test object is optically reflective this disadvantage can be solved using laser interferometer as a receiver. If the material is not absorbing water or other liquids the immersion ultrasonic technique can be applied for investigations.

6 Conclusions

The Lamb wave A_0 mode interaction with the artificial delamination type defect in the GLARE3-3/2 composite has been investigated using the one-side access air-coupled ultrasonic technique. The carried out numerical simulations and the experimental measurements have been found in a good agreement.

References

- [1] И. А. Викторов, 'Физические основы применения ультразвуковых волн Рэлея и Лэмба в технике', Наука, Москва, (1966)
- [2] A. H. Nayfeh, 'Wave propagation in layered anisotropic media', North-Holland, Amsterdam, (1995)
- [3] A. K. Mal, 'Wave propagation in layered composite laminates under periodic surface loads', Wave Motion, Vol. 10. No. 3. pp257-266, (1988)
- [4] M. J. S. Lowe, 'Matrix techniques for modelling ultrasonic waves in multilayered media', IEEE Trans. Ultrason., Ferroelect., Freq. Contr. Vol. 42. No. 4. pp525-542, (1995)
- [5] A. Demčenko, L. Mažeika, 'Calculation of Lamb waves dispersion curves in multi-layered planar structures', Ultragarsas. Vol. 44. No. 3. pp15-17, (2002)
- [6] L. Wang, S. I. Rokhlin, 'Stable reformulation of transfer matrix method for wave propagation in layered anisotropic media', Ultrasonics. Vol. 39. No. 6. pp413-424, (2001)
- [7] A. Demčenko, E. Žukauskas, L. Mažeika, R. Kažys, 'Measurement of the A_0 mode phase velocity in GLARE3-3/2 composite with air-coupled ultrasonics techniques', Insight. Vol. 47. No. 3. pp163-167, (2005)
- [8] Z. Su, L. Ye, 'Fundamental Lamb mode-based delamination detection for CF/EP composite laminates using distributed piezoelectrics', Structural Health Monitoring. Vol. 3. No. 1. pp43-68, (2004)
- [9] B. C. Lee, W. J. Staszewski, 'Modelling of Lamb waves for damage detection in metallic structures: Part II. Wave interaction with damage', Smart Mater. Struct. Vol. 12. No. 5. pp815-824, (2003)
- [10] S. C. Rosalie, M. Vaughan, A. Bremner, W. K. Chiu, 'Variation in the group velocity of Lamb waves as a tool for detection of delamination in GLARE aluminium plate-like structures', Comp. Struct. Vol. 66. No. 1-4. pp77-69, (2004)

- [11] D. N. Alleyne, P. Cawley, 'The interaction of Lamb waves with defects', IEEE Trans. Ultrason., Ferroelect., Freq. Contr. Vol. 39. No. 3. pp381-396, (1992)
- [12] N. Guo, P. Cawley, 'The interaction of Lamb waves with delaminations in composite laminates', J. Acoust. Soc. Am. Vol. 94. No. 4. pp2240-2246, (1993)
- [13] Y. Cho, D. D. Hongerholt, J. L. Rose, 'Lamb wave scattering analysis for reflector characterization', IEEE Trans. Ultrason., Ferroelect., Freq. Contr. Vol. 44. No. 1. pp44-52, (1997)
- [14] Y. Cho, 'Estimation of ultrasonic guided wave mode conversion in a plate with thickness variation', IEEE Trans. Ultrason., Ferroelect., Freq. Contr. Vol. 47. No. 3. pp591-603, (2000)
- [15] T. Hayashi, K. Kawashima, 'Multiple reflections of Lamb waves at delamination', Ultrasonics. Vol. 40. No. 1-8. pp193-197, (2002)